ELSEVIER

Flame suppression by aerosols derived from aqueous solutions containing phosphorus

T.M. Jayaweera [a,1], E.M. Fisher [a,*], James W. Fleming [b]

[a] *Sibley School of Mechanical and Aerospace Engineering, Cornell University, Ithaca, NY 14853, USA*
[b] *Combustion Dynamics Section, Naval Research Laboratory, Washington, DC 20375, USA*

Abstract

Aerosols derived from aqueous solutions containing phosphorus are investigated as possible alternatives to halon-based flame suppressants. Phosphorus-containing compounds (PCCs) have been shown to be effective flame suppressants in the gas phase; a water-based solution would provide a practical means of delivering a condensed-phase PCC to the flame. Flame suppression was characterized by measuring the global extinction strain rate of a counterflow, nonpremixed methane–air flame with and without a PCC additive. An aqueous solution of the additive was introduced as an aerosol into a heated chamber upstream of the air flow tube. A high-efficiency nebulizer produced a polydisperse spray of droplets with a Sauter mean diameter of 8 μm, as measured with a phase-Doppler particle analyzer. The droplet size distribution was nearly independent of the composition and flow rate of the liquid. Externally maintaining the reactant streams at 360 K allowed the water in the aerosol to evaporate prior to reaching the flame. Evaporation of water leaves behind residual particles for solutes that are solids at 360 K, and thus solid particulates, not droplets of solution, enter the flame zone. Comparisons of different solutions with different phase solutes were used to provide an estimate of the physical effect of particles on the flame. Three neat phosphorus-containing compounds, dimethylmethylphosphonate (DMMP), diethylmethylphoshonate (DEMP) and dimethylphosphonate (DMP) and five 1.6% molar aqueous solutions, orthophosphoric acid (OPA), phosphorus acid, phosphonic acid, methylphosphonic acid, and dimethylmethylphosphonate (DMMP), were investigated. The acid solutions (with solid solutes) all displayed similar effectiveness, and were all slightly more effective, on a per mole basis, than the DMMP solution (a liquid solute). The effectiveness of a DMMP/water solution is found to be a weighted average of the effectiveness of its constituents. Per mole of water delivered, a 1.6% molar solution of a PCC is approximately twice as effective in fire suppression compared to neat water vapor. Flame modeling calculations for the extinction condition with added gas-phase phosphorus compounds using a published phosphorus reaction mechanism grossly underpredict the total effectiveness of the compounds investigated.

© 2005 The Combustion Institute. Published by Elsevier Inc. All rights reserved.

---

* Corresponding author. Fax: +1(607)255-9410.
 E-mail address: emf4@cornell.edu (E.M. Fisher).
[1] Present address: FM Global, 1151 Boston-Providence Tpke, Norwood, MA, USA.

1. Introduction

With the restrictions on the manufacture and use of CF_3Br (halon 1301), a common fire suppressant, due to its high ozone-depletion potential, there has been widespread interest in finding a viable substitute [1–4]. A search for a drop-in replacement has not yet been successful, and as an alternative, liquid- or solid-phase agents are currently being considered. Delivering the agent as an aerosol broadens the range of potential agents available, but also makes it more difficult to predict flame suppression effectiveness. Aside from gas-phase chemical and physical effects, which occur after vaporization of the aerosol, these agents may exhibit increased flame suppression because of various phenomena related to the presence of a second phase. These phenomena include enhanced radiative heat transfer, enthalpy of vaporization, and heterogeneous reactions involving flame radicals [5–7]. Particle or droplet delivery also introduces uncertainty in the amount of agent present in the gas phase in the flame. Gas-phase loading in the flame can be reduced from the amount of condensed-phase agent in the air stream because of insufficient time for vaporization in the flame, and can be either reduced or increased when aerosol trajectories differ from air streamlines [8]. Differences in the location in the flame where the agent reaches the gas phase and possible nonuniform loading can also affect flame suppression effectiveness. In this work, a comparison is made between additives introduced as aqueous solutions leaving residual particles which then enter the flame and those that completely vaporize in the heated air stream. The experiments are designed to minimize several of the sources of uncertainty in agent loading described above.

Most of the work with solid-phase additives has focused on $NaHCO_3$ [9–12] or $KHCO_3$ [13]. These studies have all shown these powders to be more effective than CF_3Br at fire suppression. The effectiveness is highly dependent on the size of the particles, with smaller particles having a greater effect than larger ones on a per mass basis. This difference is attributed to the large particles not being completely consumed in the flame zone. The high level of effectiveness from these small particles is believed to be due, at least in part, to a chemical effect of the agent in the gas phase [5,12].

In the liquid phase, water mists have been gaining in popularity, due to their relatively high level of effectiveness and zero toxicity [8,14–17]. A water mist has been shown to be more effective, on a per mass basis, than CF_3Br in nonpremixed counterflow flames [17]. However, water acts primarily as a physical agent in suppressing the flame. A variation of the traditional water mist is an "enhanced"

water mist: a water solution containing a compound that, through effects on flame chemistry, increases the fire suppression effectiveness over that of pure water [18–20]. A concern with adding a chemical agent is that toxicity of the solution will be higher than of pure water. However, as the chemical agent's effectiveness is supplemented by that of the water accompanying it in an enhanced water mist, its required concentration may be acceptably low from the standpoint of toxicity.

A few experimental studies have been done with enhanced water mists, namely water solutions of NaOH or NaCl [19–21]. These show enhancements of flame suppression compared to pure water. For example, a water mist enhanced with 18% NaOH by mass was shown to be several times more effective than pure water in an opposed-jet, nonpremixed methane–air flame [21]. The mechanism by which an enhanced water mist results in improved suppression over neat water is believed to be due to several factors. In addition to the physical effect of the water, there is likely a chemical effect by the solute, and possibly also a physical effect from the droplets or residual particles [19,21]. The relative magnitudes of these effects have not been determined. In our study, the flame suppression effectiveness of aerosols derived from water solutions containing phosphorus was investigated experimentally, and contributions of the chemical and physical effects were evaluated.

Phosphorus compounds have been studied previously in the gas phase and shown to be highly effective flame suppressants [22–25]. Since low vapor pressure hinders the introduction of many phosphorus-containing compounds (PCCs) in the gas phase, their use in practical fire fighting situations is limited. However, experimental and numerical studies [22,26–28] have shown that the effectiveness of different gas-phase PCCs is similar, expanding the range of PCCs available. This similarity of effectiveness is supported by the proposed mechanism by which PCCs suppress the flame: they are converted to phosphorus-containing radicals, such as HOPO and $HOPO_2$, which catalyze the recombination of the important combustion radicals, H, OH, and O [23,25,29]. This process slows the overall reaction rate and thus suppresses the flame. Earlier studies used laser-induced fluorescence to measure OH radical levels in a nonpremixed flame with and without dimethylmethylphosphonate [24,30]. These measurements show a decrease in the OH level with the addition of this PCC, supporting the hypothesis of catalytic radical recombination. With the inhibition resulting primarily from the phosphorus atom, the use of PCC solutions, as enhanced water mists, is a possible means of getting the phosphorus into the flame.

In the current study, a nonpremixed methane–air flame was used to investigate the effectiveness of several PCCs. These compounds are delivered into the air stream in the vapor phase, as a fine mist of neat liquid, or as a fine mist of aqueous solution. Neat liquids and aqueous solutions involving liquid solutes, such as the PCC dimethylmethylphosphonate (DMMP), are expected to evaporate fully before the flame. For other compounds introduced as droplets of the aqueous solutions with solid solutes, a small residual particle is expected to remain upon evaporation of the water from the solution droplet. Assuming all of the phosphorus compounds have similar chemical fire suppression effectiveness once they are in the gas phase, fire suppression effects due to the particle phase can be investigated.

Experiments were performed using an opposed-jet burner apparatus [31]. This configuration has been used extensively with experimental, numerical, and analytical techniques to evaluate the performance of flame suppressants [4,32,33]. The counterflow configuration is useful in studying flame-suppressing additives as the flame is thermally isolated and quasi-one-dimensional along the centerline [34,35]. Flame strength can be characterized by the global strain rate at extinction [36,37].

Extinction calculations were also performed using OPPDIF [38], part of the Chemkin software package [39]. These calculations used a proposed phosphorus mechanism and investigated the gas-phase suppression effect of three phosphorus compounds. These calculations were done to further elucidate differences in the suppression effectiveness observed between PCCs delivered in the gas phase and those in the particle phase.

2. Experimental method

The flame suppression effectiveness of several PCCs, introduced into the burner system either in the vapor phase or as droplets of neat liquid or aqueous solution, was investigated. The compounds are listed

with their CAS number and chemical structure in Table 1, along with the form in which they were introduced into the burner system. The compounds studied were: distilled water, dimethylmethylphosphonate, diethylmethylphosphonate (DEMP), dimethylphosphonate (DMP), orthophosphoric acid (OPA), methylphosphonic acid (MPA), phosphonic acid, and phosphorous acid. DMMP, DEMP, DMP (all 97% pure) and MPA (98% pure) were supplied by Aldrich Chemical Company, phosphonic and phosphorous acids (each 97% pure) were supplied by Alfa Aesar, and OPA was supplied as a premixed aqueous solution from Aqua Solutions. Each of the phosphorus acids was in a 1.6% molar solution in distilled water, and DMMP was introduced both in a 1.6% aqueous solution and as a neat compound, in separate experiments. As shown below, essentially all water and DMMP evaporate before the oxidizer mixture leaves the burner nozzle. In the case of the acid solutions, a solid residual particle remains, while for DMMP and water, the mixture entering the flame is entirely gas phase. The acid compounds were chosen because they have been seen, through in situ sampling and GC/MS analysis [40], to be decomposition products of DMMP, a PCC shown to be an effective flame suppressant [22,23]. These compounds are also attractive because of their low heating value and because, unlike many PCCs, they are not believed to be neurotoxic.

For compounds introduced in the liquid phase, the experimental apparatus consists of a nonpremixed counterflow burner equipped with a system for adding the liquid agent into the oxidizer stream: a nebulizer mounted in a large chamber, leading into temperature-controlled tubing. The apparatus is shown in Fig. 1. Its key features are small droplet size, large residence time of the reactant stream under temperature-controlled conditions, and the availability of an accurate procedure for measuring losses to surfaces within the feed system. These features lead to a well-characterized state of the reactant mixture at the exit of the burner tube, and well-defined gas-phase loading of agent at the flame, as documented below. In

Table 1
Compounds used

| Compound	Form	CAS number	Molecular formula
Orthophosphoric acid (OPA)	Aqueous solution	7664-38-2	$P(=O)(OH)_3$
Phosphorous acid	Aqueous solution	10294-56-1	$P(OH)_3$
Phosphonic acid	Aqueous solution	13598-36-2	$P(=O)(H)(OH)_2$
Methylphosphonic acid	Aqueous solution	993-13-5	$P(=O)(CH_3)(OH)_2$
Distilled water	Neat liquid, vapor	7732-18-5	H_2O
Dimethylmethylphosphonate (DMMP)	Neat liquid, vapor, aqueous solution	756-79-6	$P(=O)(CH_3)(OCH_3)_2$
Diethylmethylphosphonate (DEMP)	Neat vapor	683-08-9	$P(=O)(CH_3)(OCH_2CH_3)_2$
Dimethylphosphate (DMP)	Neat vapor	813-78-5	$P(=O)(OCH)_2(OH)$
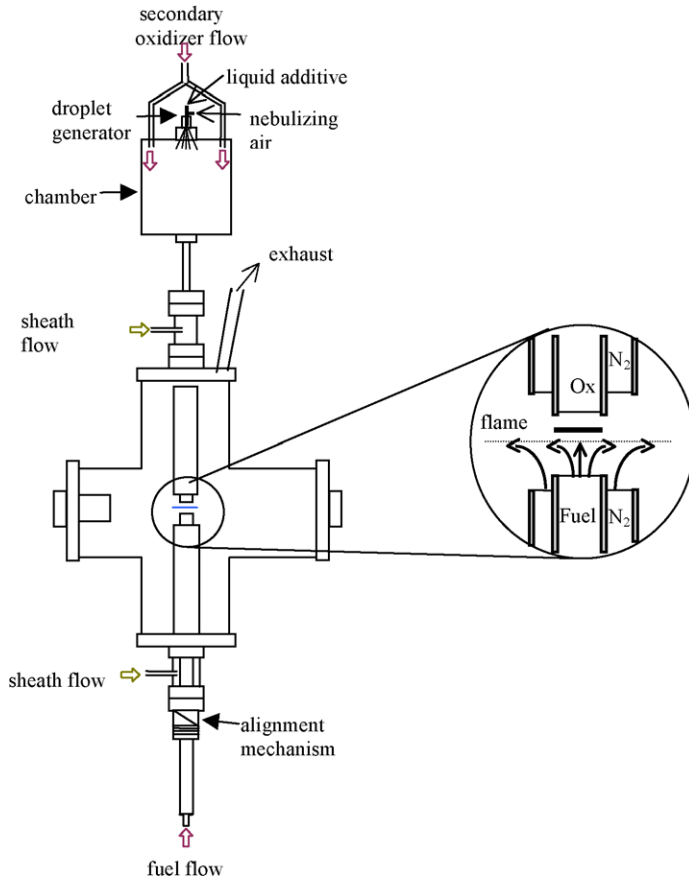
Fig. 1. Schematic of experimental apparatus with opposed-jet burner, droplet generator, and chamber.

the case of additives introduced in the vapor phase, the nebulizer and chamber are replaced by a syringe pump and further length of heated tubing, as previously described [22].

2.1. Burner

The flame is produced approximately 2 mm on the oxidizer side of the stagnation plane of counterflowing streams of fuel and oxidizer. This opposed-jet burner geometry has been detailed previously [22]. As in previous experiments, the reactant nozzles are straight glass tubes (0.98 cm i.d.) with a separation distance of 0.95 cm. Methane (99% pure) fuel flows from the lower nozzle and the oxidizer, a primary standard mixture of $21 \pm 0.2\%$ O_2 with N_2 balance, flows through the upper nozzle. All gases were supplied by MG industries. The temperature of the reactant streams 10 cm upstream from the exit of the nozzles are actively maintained at 360 ± 1 K.

The relative flame strength is characterized by the global strain rate at extinction, calculated using the following expression:

$$a_q = \frac{2V_O}{L} \left(1 + \frac{V_F}{V_O} \left(\frac{\rho_F}{\rho_O} \right)^{1/2} \right). \tag{1}$$

In Eq. (1), L refers to the separation distance between the nozzles, V is the average stream velocity at extinction, ρ is the stream density, and the subscripts O and F refer to oxidizer and fuel, respectively. Plug flow boundary conditions at the nozzle exit are assumed. This expression, derived by Seshadri and Williams [41], is referred to as the global extinction strain rate. To determine suppression effectiveness of the added compounds, the global extinction strain rate was measured as a function of dopant loading. The resulting extinction strain rates a_q are normalized by the undoped value, a_{q_0}, which was found to be 340 s^{-1} in the absence of the heated chamber described in the next section and 322 s^{-1} when the chamber was present (each with a day-to-day variation of less than 4%). Although this difference in absolute extinction strain rate is significant, the normalized extinction strain rates obtained with the two configurations were not significantly different.

The extinction strain rate is determined at a fixed nozzle separation, L. The reactant velocities are increased until the critical strain rate is achieved and the flame is extinguished. In most studies [4,42], both the fuel and the oxidizer velocities are increased proportionally such that the flame or stagnation plane is maintained near the center of the burner. Because the addition of a liquid-phase dopant is via a mass-flow syringe pump, changing the doped reactant flow rate would change the dopant loading, leading to transients of a fairly long time scale (several minutes). This difficulty is circumvented by performing extinction measurements holding the doped reactant (oxidizer) stream fixed, and only varying the undoped (fuel) stream flow rate. The flame and stagnation plane move in this method, but for a range of known flame positions, the global extinction strain rate was found to agree within ±2% [22]. A validation of this technique with residual particles present was performed for the current study.

2.2. Generation and characterization of droplet mist

A small glass nebulizer is used to deliver the liquid-phase dopant to the oxidizer stream as a fine mist of droplets. A high-efficiency nebulizer (HEN), a Meinhard® nebulizer, is detailed in Fig. 2. Liquid is introduced via a programmable syringe pump. Part of the oxidizer stream is supplied as the nebulizing gas at a flow rate of 1.00 SLM. This flow rate allows for sufficient aerodynamic breakup of the liquid stream into a fine mist. The HEN is mounted at the top of a large heated chamber (15 cm i.d., 18 cm long) located approximately 75 cm upstream of the flame. Unfortunately, the presence of the chamber induced flow fluctuations that perturbed the flame. To dampen these fluctuations, a small diameter (3.2 mm i.d., 7.6 cm long) tube was placed between the chamber and the reactant flow tube.

In order to make valid comparisons between different compounds at several loadings, it is important
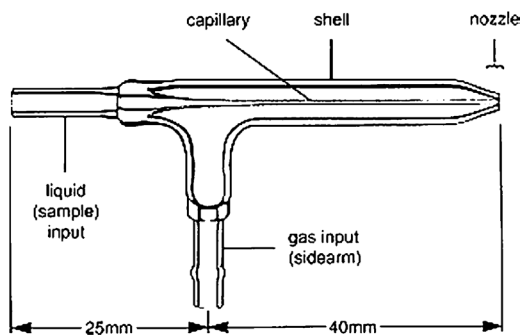
for the droplets produced in each case to be similar. The droplets should also be small enough so that they will completely evaporate prior to reaching the flame. Measurements of droplet diameters were performed with a phase-Doppler particle anemometer (PDPA, Dantec FlowLite Fiber PDA). The HEN was not mounted in the burner apparatus for the PDPA measurements; rather, it was mounted in an enclosed chamber with good optical access. Droplet diameters were measured for a variety of concentrations and flow rates of phosphorous acid, as well as for a single set of conditions for water, DMMP, OPA, MPA, and phosphonic acid. PDPA measurements were performed 1.3 cm downstream of the HEN tip, with 1.00 SLM of nebulizing gas. Typical histograms for two different cases are shown in Figs. 3a and 3b; the certainty of the PDPA measurement is ±2 μm for the optical configuration and processor settings used. As can be seen in the histogram, all of the droplets are
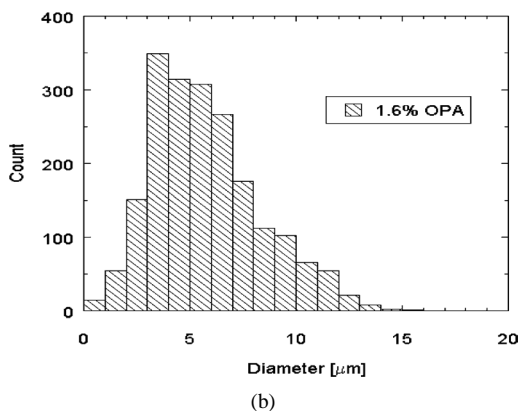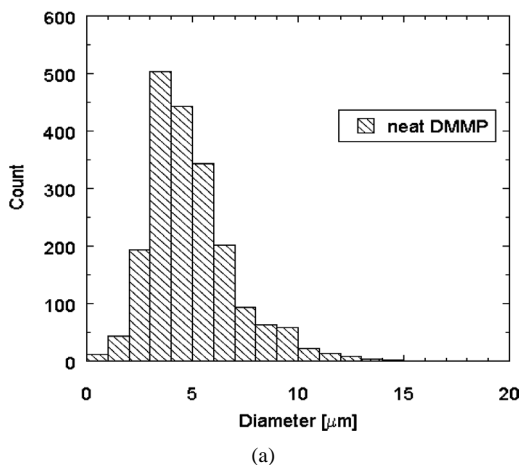

(a)

(b)

Fig. 3. PDPA measured size histogram for 2000 droplets of two different PCCs, measured 1.3 cm downstream of HEN exit. The liquid flow rate for both compounds was 25 μl/min with 1.00 SLM of nebulizing air. (a) Neat DMMP (b) 1.6% (molar) aqueous solution of OPA.

Fig. 2. Schematic of the high-efficiency nebulizer (HEN) droplet generator, provided by Meinhard and Associates.

Table 2
The droplet diameter size distributions at 25 μl/min obtained from PDPA measurements fit to a log-normal distribution

Compound	A (dimensionless)	x_0 (μm)	α (μm)
Neat H$_2$O	162.9	1.625	0.688
7.5% P(OH)$_3$	216.8	1.844	0.514
7.5% MPA	235.0	1.833	0.469
7.5% H$_3$PO$_3$	216.8	1.844	0.514
4.3% DMMP	169.4	1.611	0.662
1.6% OPA	170.6	1.742	0.662
Neat DMMP	213.9	1.566	0.589

Note. The parameters given fit the form $A\exp(-(x-x_0)^2/\alpha^2)$, and were evaluated using a least-squares method.
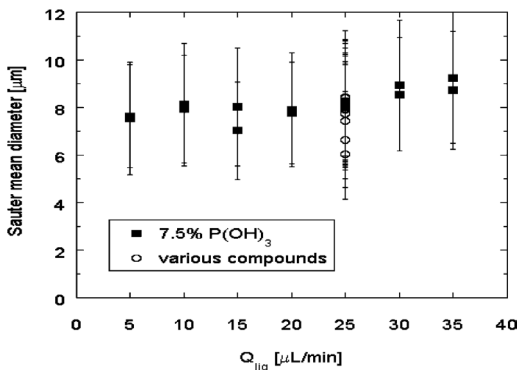

Fig. 4. PDPA measured Sauter mean diameter, 1.3 cm downstream of HEN exit, as a function of liquid flow rate. Under conditions in this paper for the 7.5% phosphorous acid solution, 25 μl/min corresponds to a total loading of 1.49%. The various compounds tested were 7.5% phosphorous acid, 1.6% orthophosphoric acid, 7.5% phosphonic acid, 7.5% methylphosphonic acid, neat DMMP, 4.3% DMMP, and neat H$_2$O. All concentrations are molar based in an aqueous solution. Error bars represent one standard deviation in the diameter measurement of 2000 droplets.

less than 20 μm in diameter and the size distributions for the two solutions are very similar. Size distributions were fit to a log-normal distribution using an equation of the form $A\exp(-(x-x_0)^2/\alpha^2)$. The fit parameters were determined using a least-squares method and are given in Table 2 for all the compounds tested. The Sauter mean diameters from all the different cases are plotted in Fig. 4. The error bars represent one standard deviation of the droplet size determination.

2.3. Evolution of droplet mist

For droplets of neat liquids and DMMP/water solutions, complete evaporation upstream of the exit of the oxidizer nozzle is ensured by high temperatures and long residence times. The chamber is heated electrically, while the temperature of the gas in the burner tube is actively controlled to 360 ± 1 K by electric heating of the surrounding sheath gas. The average residence time of the droplets is several seconds, while a simple d^2 analysis [43] of the evaporation rate for the maximum droplet size predicts that pure DMMP or water droplets should evaporate entirely within a few milliseconds within the chamber. To confirm complete evaporation, a He–Ne laser beam was passed through the reactant stream just below the exit plane of the oxidizer nozzle, and the off-axis forward direction was scanned by eye for scattered light. For neat solutions, there was no observable scattered light, consistent with the complete evaporation of the liquid at this point.

For droplets of phosphorus acid solutions, which should produce residual solid particles upon evaporation of water, little quantitative information is available on evaporation rates. However, it is expected that these evaporation times are comparable to those for neat liquids, and that the much longer residence times upstream of the burner nozzle are sufficient to achieve phase equilibrium between the residual particle and the surrounding gas stream. Whether the compounds under consideration exhibit deliquescence (producing dry residual particles) or retain some water even at low relative humidity is not known. As calculated from the reactant flow rates, the relative humidity of the air stream is only 2.4% under burner exit conditions, and thus the amount of water retained in the particle at equilibrium is likely to be small if not zero.

For all compounds, active temperature control of the reactant streams is crucial. The agent-doped oxidizer stream is heated externally to maintain its temperature at 360 K. The enthalpy of vaporization of the water is not supplied by the flame but from external sources, and thus does not contribute to the flame suppression process for the liquid droplets in these experiments. The apparatus is designed to produce a well-defined state for the oxidizer stream at the nozzle exit: phase equilibrium at 360 K, with all phases traveling at the same velocity. This well-defined boundary condition at the nozzle exit is highly desirable for computational modeling.

When residual particles are present, their ability to follow gas streamlines in a decelerating flow is size dependent. Size also determines whether in-flame vaporization is fast enough to release the entire mass of the added agent into the gas phase. Clearly, small particles are desirable to produce well-defined gas-phase agent loadings for both of these reasons. The residual particle diameter can be estimated from the measured droplet size distribution by assuming that each droplet loses all of its water and becomes a spherical particle with density equal to that of the pure solid PCC. With this assumption, evaporation of the drops for these aerosols yields a Sauter mean particle diameter

of ∼3 µm and a maximum particle diameter of 7 µm. Although rapid heating of solution droplets has been shown to produce highly nonspherical residual particles [44], the assumption of a spherical particle gives conservative results for both drag and vaporization rates. The current estimate of particle size will not be conservative, however, if significant coalescence of droplets occurs downstream of where the droplet size distribution was measured.

Stokes numbers represent the ratio of particle response time to flow residence time. At typical extinction strain rates in this burner, Stokes numbers for the estimated mean and maximum particle size for 1.6% OPA solution are calculated to be 0.02 and 0.1, respectively. These low values indicate that particles are able to follow the gas streamlines, avoiding the complications of nonuniform loading described by other investigators [8]. The estimated particle sizes are well below 30 µm, the diameter for critical damping for our flow conditions, determined using the expression developed by Li et al. for estimating critical damping in this flow field configuration [45]. Thus the particles should not oscillate in the flowfield.

Another indication of how well the particles follow the gas streamlines is obtained from a comparison of the drag force (assuming Stokes flow) with either the gravitational force or the thermophoretic force. The terminal velocity for 8-µm particles (resulting from 20-µm droplets), relative to the gas flow, is of the order of 1.5 mm/s, and for 3-µm particles it is 0.2 mm/s. A thermophoretic velocity can similarly be calculated, by equating the thermophoretic force to the drag force. This velocity is constant for small particles with a Knudsen number greater than ∼1 [46]. At smaller Knudsen numbers, the thermophoretic velocity decreases and becomes dependent on the thermal conductivity of the particle. Thus, using a small particle that satisfies the Knudsen number constraint gives a conservative estimate of the thermophoretic velocity. The thermophoretic velocity at the location of the maximum temperature gradient can be derived using temperature and velocity profiles from calculations performed under similar conditions [30]. This velocity, for a 0.1-µm particle, was found to be 0.145 m/s, or about 25% of the local gas velocity. Although this relative value appears significant, its effect on particle trajectories and dopant delivery is small because thermophoresis is significant only when particles are very small, i.e., near the end of the vaporization process. The magnitude of this effect can be seen for NaCl particles (for which the physical properties are well known). Thermophoresis is calculated to shift the location of complete evaporation of a 0.1-µm NaCl particle upstream by only about 2 µm. This shift is negligible when compared to a calculated flame FWHM of around 1.7 mm. Thus, neither gravitational nor thermophoretic forces should strongly influence the particle trajectories for the flame conditions reported here.

Viewing of scattered laser light, as described previously, provides information about the completeness of particle vaporization in the flame. Experiments were performed with a mist of 1.6% OPA introduced by the HEN, with a strain rate 10% below the extinction value. Scattered light was observed when the laser beam was positioned just below the exit plane of the oxidizer nozzle confirming the ability to detect residual particles. No scattered light was observed when the laser was positioned below the flame region, indicating that the particles are small enough to be consumed in the flame. At this position, care was taken to ensure that the laser beam was between the stagnation plane and the flame: scattered light was observed in this region at the same reactant flow rates, but with no flame present.

2.4. Wall losses

The chamber housing the HEN was designed to minimize wall losses. The liquid spray exits the HEN in a small-angle cone (∼15° half-angle), and enters a large chamber that has a supplemental oxidizer stream entering near the edge. The use of this chamber did not prevent all wall losses, however. For the solutions, some droplets or residual particles were still lost to the walls. To quantify the amount of acid PCC lost, the following rinsing procedure was used. A known amount of OPA, in the form of a 1.6% water solution, was sprayed into the apparatus under the same conditions used for the extinction experiments. The chamber and all tubing downstream were then rinsed with a known amount of distilled water. The pH of the wash was measured using an Accumet pH probe, and the concentration of OPA was determined from its dissociation constant. The amount of acid recovered was compared to the amount entering the HEN, and losses were calculated to determine the net amount delivered to the flame. Several different air and liquid flow rates were tested. PCC losses were found to be $13.8 \pm 0.6\%$ of the initial amount delivered. This correction, measured with OPA, is applied to all aqueous solutions of phosphorus acids. Since the initial droplet distributions for all compounds producing residual particles are very similar, the assumption of the same loss is reasonable. It is assumed that losses occur only for the acid PCC, and that any accompanying water that impinges on the walls is subsequently evaporated.

For liquids not producing residual particles, zero losses are assumed on the basis of two observations. First, as observed previously for vapor-phase DMMP delivery [22], no trend in extinction measurements was observed as a function of time, suggesting that

wall adsorption/desorption processes were negligible or had reached steady state. Secondly, when the DMMP flow was abruptly shut off, the flame rapidly returned to its undoped blue color on a time scale consistent with the average gas-phase residence time in the heated chamber. Wall deposits, if they had existed, would be expected to vaporize in the presence of a lower gas-stream dopant concentration and delay the return of the undoped appearance of the flame. In previous experiments with vapor-phase DMMP and no heated chamber [22] the return of the blue color had been virtually instantaneous. Consistency of DMMP extinction results obtained with the two systems, reported under Section 3, provides further evidence that wall losses are negligible in the HEN system.

2.5. Calculations

Extinction calculations were performed using the OPPDIF code, from the Chemkin II suite [38]. OPPDIF is not designed to incorporate multiphase reactants, such as particle-phase dopants. There is no means of calculating radiative losses or effects due to surface chemistry. Nor is there a means of accounting for differences between particle and gas velocities. Therefore, OPPDIF is used in these studies to calculate the differences in effectiveness between different phosphorus-containing compounds based only on their gas-phase effects. Computationally, all compounds are treated as being in the gas phase, regardless of the phase in which they exist in the experiment.

The phosphorus mechanism is employed by Glaude et al. [47] and was developed for DMMP combustion. OPA and phosphorous acid are also included in this mechanism. The GRI-Mech 3.0 [48], excluding nitrogen chemistry, was used for the hydrocarbon combustion. Mixture-averaged diffusion velocities were used, and thermal diffusion was neglected. A potential flow boundary condition with a centerline axial velocity of twice the measured volume averaged velocity was used. This set of velocity boundary conditions was determined by MacDonald et al. [30] to best match experimental results of [OH] measurements with this particular burner.

The extinction calculations were performed in a manner similar to that described by Pitts et al. [49]. That is, extinction was approached with small incremental steps in flow rates of the fuel and oxidizer (of at most 0.01 SLM for the fuel). The flow rates were changed such that the position of the flame remained constant. Subsequent calculations with a higher velocity were restarted from previous solutions to decrease computational time. The extinction strain rate was determined to be the highest strain rate at which a solution was found. For all the calculations, 250 ppm of PCC and/or 1.54% H_2O was added.

3. Results

Extinction measurements were performed for H_2O and DMMP as neat compounds. Fig. 5 presents the normalized global extinction strain rate obtained when the dopant enters the burner system as a liquid spray, comparing it to results when the dopant enters as a vapor. The loadings are calculated, for all cases, assuming the dopant is completely evaporated. For the vapor-phase tests, the dopants were added, via syringe pump, into a heated reactant line upstream of the oxidizer flow tube. The vapor-phase tests for DMMP were performed and reported earlier [22]. The same additive loadings were investigated here with the dopant introduced into the burner system in the liquid phase, using the HEN. The absence of scattered laser light indicated complete evaporation of the H_2O and DMMP droplets. Fig. 5 demonstrates that the normalized global extinction strain rate is independent of the initial phase of the additive. The agreement between extinction measurements for the two methods of dopant introduction is consistent with complete evaporation of the neat liquid droplets with the enthalpy of vaporization supplied externally rather than from the exothermicity of the combustion reaction.

The suppression effectiveness of H_2O vapor determined here can be compared to literature values obtained with reactants at a slightly lower temperature. Lentati et al. numerically investigated the effect of various concentrations of water vapor added to a nonpremixed methane–air flame with reactants at 300 K [8]. A roughly linear behavior is predicted with water addition, with a 25% reduction in extinction strain rate by a saturated air stream at 300 K
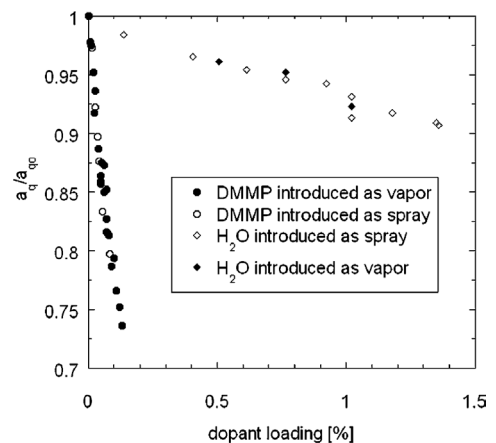

Fig. 5. Normalized global extinction strain rate of neat DMMP and H_2O, as a function of dopant loading. The dopant was introduced either as a spray via the HEN or in the vapor phase upstream of the oxidizer flow tube. Loadings are given as the mole fraction of dopant in the oxidizer stream assuming complete vaporization.
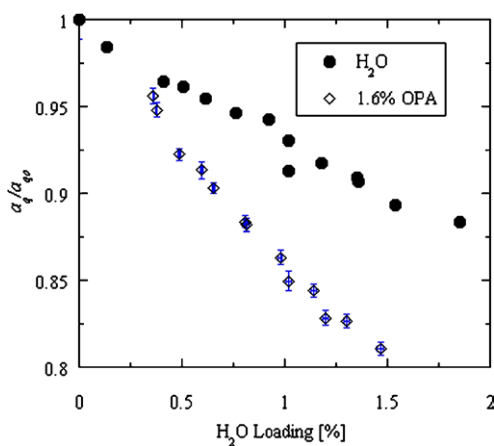
Fig. 6. Comparison of normalized global extinction strain rate as a function of H_2O loading (assuming complete vaporization) due to addition of neat H_2O and a 1.6% (molar) aqueous solution of OPA. Error bars on OPA data represent one standard deviation due to scatter in extinction measurements (δy_i) and uncertainty in loading (δx_i).

(water loading 3.51%). Experiments have also been performed by Lazzarini et al. [21] with saturated water vapor at the same temperature, finding only a 12% reduction in extinction strain rate. Our experimental results, shown in Fig. 5 for 4 to 40% of the amount of water in a saturated air stream at 300 K, indicate that the extinction strain rate is linear over this range. These results are in reasonable agreement with Lentati's calculations over the range in which they overlap. It should be noted, however, that the present measurements were made with the reactants at 360 K, while the numerical predictions assume 300 K. A linear extrapolation of the current experimental results to 3.51% water loading gives a 24% reduction in extinction strain rate, which agrees well with Lentati's calculated value but it is twice Lazzarini's measured value.

Experiments were performed comparing H_2O to an aqueous solution of 1.6% OPA. The results are given in Fig. 6, with the normalized extinction strain rate plotted as a function of molar loading of the H_2O only. For the case of the PCC, the H_2O loading is calculated by subtracting the amount of phosphorus compound (1.6%) from the total dopant loading. It also assumes that all of the water is delivered to the flame. Error bars in the OPA data set represent uncertainties of one standard deviation. The y-error bars, between 1 and 2%, are an appropriate combination of uncertainties in a_q and a_{q0}, each of which is found empirically as the standard deviation of eight repeated measurements. The x-error bars, between 1 and 5%, are derived from the uncertainties of flow rates of dopant and oxidant, and from the standard deviation of the measured dopant loss rate.

The absolute value of the slope of Fig. 6 represents the effectiveness of the suppressant [50,51]. The uncertainty in slope can be calculated from the uncertainties in the measured quantities contributing to it, using standard methods [52]. Two types of uncertainty must be considered: those affecting each data point randomly, and those affecting all data points in a given set in the same way. The truly random uncertainty contributions are responsible for the scatter in a given data set, and are described above and displayed as error bars in Fig. 6. For the purposes of calculating a slope, uncertainties in the x coordinate (loading) were converted to an equivalent y uncertainty, as recommended by Bevington [52]. Then the random uncertainties in the individual data points were combined, contributing an uncertainty of at most 1.6% to the slope. In addition to this uncertainty it is important to include the uncertainty in the solute concentration (1.8%), which has the same fractional effect on the loadings of all data points obtained from a given batch of aqueous solution. When these errors are included, the uncertainty in the slope is still under 2.5% for all cases presented here. This calculated uncertainty was verified by comparing the slopes for two sets of extinction measurements for OPA obtained with different solute mixtures; the two slopes agreed within the calculated uncertainty. Not included in this analysis is the error in extinction strain rate due to the method by which extinction is approached ($\pm 2\%$; see Section 2.1). Because of the choice of conditions, this error is nonrandom and has the same value at a given strain rate, regardless of the choice of suppressant. Thus it has no effect on the relative effectiveness of the different suppressants.

A linear regression on the slopes in Fig. 6 with a fixed y-intercept indicates that 1.6% of phosphorus approximately doubles the effectiveness of pure H_2O vapor, per mole of H_2O delivered. Thus, an enhanced water mist can substantially improve the suppression performance over that of pure water vapor, without introducing large quantities of a chemical substance. This result has also been observed by other researchers who have investigated the suppression effectiveness of enhanced water mists doped with sodium-containing compounds [18–20,53].

To test whether the chemical structure of the parent phosphorus compound is important, several PCCs were introduced to the flame and suppression effectiveness was compared. The compounds tested were three neat phosphorus compounds (DMMP, DEMP, DMP), and five 1.6% (molar) aqueous solutions (DMMP, OPA, MPA, phosphorous acid, and phosphonic acid). The neat compounds were introduced using a method described earlier [22] and the aqueous solutions were introduced into the burner system via the HEN. Flame extinction results are given in
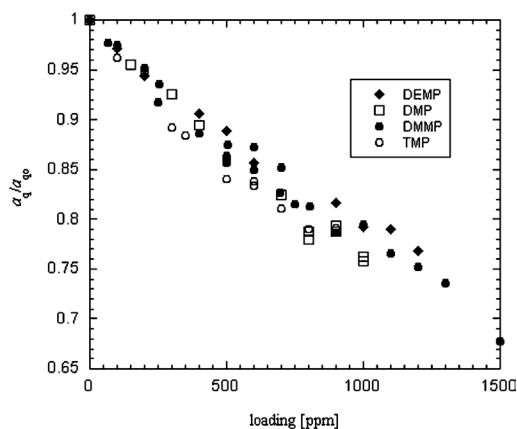
Fig. 7. Comparison of normalized global extinction strain rate as a function of phosphorus loading for several different phosphorus-containing compounds, namely trimethylphosphonate (TMP), dimethylmethylphosphonate (DMMP), dimethylphosphate (DMP), and diethylmethylphosphonate (DEMP). These compounds are all introduced in the neat form, and enter the flame in the vapor phase. TMP and DMMP results are from [22] and are included here for comparison.
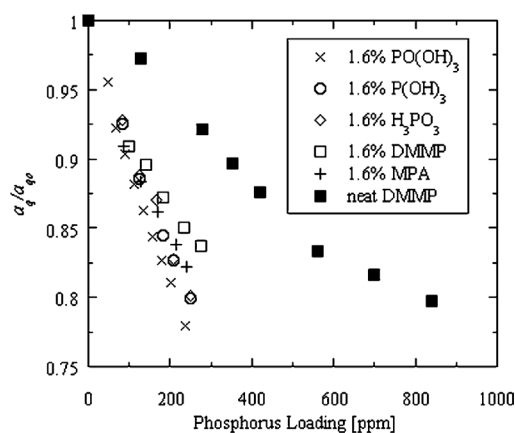

Fig. 8. Comparison of normalized global extinction strain rate as a function of phosphorus loading for several different phosphorus-containing compounds. DMMP was introduced as a neat compound via the HEN. All other compounds, including 1.6% (molar) aqueous solutions of DMMP, orthophosphoric acid, phosphorous acid, phosphonic acid, and methylphosphonic acid, are introduced into the burner system via the HEN. The phosphorus loadings for the acid solutions have been corrected for wall losses.

Figs. 7 and 8, for the compounds introduced into the burner system as neat liquids and aqueous solutions, respectively. The extinction results are plotted versus the "phosphorus loading," or the mole fraction of phosphorus-containing molecules in the oxidizer stream expressed in ppm assuming complete vaporization of the additive. Since each PCC molecule

Table 3
Global extinction strain rate reduction by the compounds tested: slope of normalized extinction strain rate vs agent loading

Compound	Slope (ppm^{-1})	Corrected slope (ppm^{-1})
Neat		
DMMP	223	267
TMP	269	311
DMP	247	278
DEMP	204	255
1.6% *aqueous solution*		
Orthophosphoric acid (OPA)	997	996
Phosphorous acid	835	840
Phosphonic acid	814	818
Methylphosphonic acid	792	808
Dimethylmethylphosphonate (DMMP)	654	697

Note. The uncertainty in the slope is 2.5% (see text). The TMP data were reported in an earlier paper [22] and are included here for reference. Values for the corrected slope are derived by considering the heating value of the indicated compounds (see text).

contains a single phosphorus atom, these loadings represent the number of moles of phosphorus atoms per total moles in the oxidant mixture. Neat DMMP is included with the aqueous solutions for comparison. For the DMMP/water solution, the phosphorus loading is the mole fraction of DMMP in the oxidizer stream, assuming total vaporization of DMMP and water. Here, as well as for all of the neat compounds, zero wall losses are assumed. For the phosphorus acid solutions, the phosphorus loading is calculated as for the DMMP/water solution, and then reduced by 13.8% to correct for wall losses. (See Section 2.4.)

Fig. 7 shows that the neat phosphorus compounds are all similarly effective. There is total scatter between the different compounds of about 20%. The results from this study, indicating that the form of the parent compound is relatively unimportant in flame suppression, are used when examining the effect of aqueous solutions containing phosphorus. The slopes for the curves in Fig. 7 are given in Table 3.

The results in Fig. 8 fall into two groupings: the neat substance, DMMP, and the substances introduced into the burner system as water solutions. Compared to the neat DMMP, the water solutions have steeper slopes, implying higher flame suppression effectiveness per atom of added phosphorus. This difference is due to the flame suppression contribution from the water in the solution. The results for the 1.6% solution of DMMP can be used to assess whether DMMP and water have additive effects. Linear regressions of the data in Fig. 5 give values of the slopes of the normalized extinction strain rate vs

mole fraction for neat DMMP and H_2O. A weighted average of these two numbers yields a predicted "effectiveness" of a 1.6% solution of DMMP in water to be only 5% more than the measured effectiveness of the solution. Thus, one can assume that within uncertainty, additivity of effectiveness is valid under the conditions of the current experiment. However, it is expected that synergistic rather than additive behavior will be seen at high H_2O loadings, as the effectiveness of chemical agents has been observed to increase with decreasing temperatures [30,54]. In our experiments, the change in the adiabatic flame temperature by the amount of water added would result in only a small change in the extinction strain rate. Addition of 1.5% H_2O changes the adiabatic flame temperature by only 20 K; according to previous work [50], this change would increase the effectiveness of the chemical compound by roughly 10% compared to addition to a flame without an inert dopant. It should be noted that due to considerable scatter in the cited work, particularly in the range of interest for this work, there is uncertainty in the magnitude of this synergistic effect. Nonetheless, synergy implies that the effectiveness of the solution should be more effective that the weighted average of the neat compounds, not nearly equally as effective as observed here for the 1.6% DMMP solution. Further work at higher H_2O loadings is needed.

All of the acid solutions studied (OPA, MPA, phosphonic acid, and phosphorous acid) exhibit similar reduction of the global extinction strain rate, per mole PCC added to the air stream. There is a maximum difference of about 22% in the measured effectiveness, based on a comparison of the slopes. When the data for the DMMP solution are included, the spread is larger: there is a maximum difference of 42% in slopes in the set of water solution data (between DMMP and OPA). These slopes, along with corrected slopes described below, are given in Table 3. The possible significance of the difference between results for the DMMP solution (which vaporizes entirely) and for phosphorus acid solutions (which produce residual particles) will be discussed later.

The spread in suppression performances for the phosphorus acid solutions studied is outside the estimated experimental measurement uncertainty. Chemical and physical differences in the phosphorus compounds could result in differences in fire suppression effectiveness. Such differences in the added compounds, including differences in heating values, differences in the kinetics leading to the formation of the phosphorus-containing species that participate in radical recombination cycles, and specific characteristics of any residual particles such as vaporization rate or

radiative properties, may also contribute to the suppression difference.

Additive species, or portions thereof, that contain hydrocarbons, will to some extent promote the flame due to their associated heating values. Extinction strain rate measurements were performed with a small amount (400 ppm) of iso-octane added to the air stream of a methane/air nonpremixed flame, resulting in a promotional effect of 4% [22]. To estimate the magnitude of the promotional effect of the fuel content of other additives considered in this work, the hydrocarbon content of the PCC is compared to that of the iso-octane. The additives' heating values were compared (on a molar basis) to that of iso-octane, allowing the measured PCC effectiveness to be corrected for the fuel contents effect (assuming constant promotional effect per unit heating value). In addition to the contribution of the hydrocarbon groups, there is some contribution to the total heating value of the PCC species due to the phosphorus atom itself. The heating values of PCCs in this study were calculated assuming that the phosphorus product is the thermodynamically preferred species, P_4O_{10} [55]. Correcting for heating value effects brings the phosphorus-based acids into better agreement with each other. The corrected slopes, given in Table 3, represent the slopes corrected for the heating value of the different compounds. After correction, OPA is still some 20% more effective than the other acid solutions. The source of this increased effectiveness is uncertain but may be related to the nature of the residual particles from this solution.

The difference between the DMMP solution (which vaporizes entirely) and the phosphorus acid solutions (which produce residual particles) suggests an enhanced effectiveness role for the particles. An enhanced radiative heat loss from flames due to the addition of inert particles has been predicted and observed experimentally in premixed flames [7]. Other effects, such as enthalpy of vaporization and reactions on the particle surface, may also contribute to an increase in effectiveness from the addition of particles. In the current experiments, particles that enter the flame are consumed in it. Thus, all of the phosphorus atoms are eventually available to participate in the gas-phase catalytic removal of the flame radicals H, O, and OH. Otherwise, one would expect a decrease in effectiveness resulting from the presence of particles. As the data in Table 3 indicate, all of the phosphorus-based acid solutions that produce residual particles are more effective than the DMMP solution that does not form particles. Thus, these results are consistent with a predicted increase in suppression effectiveness for the residual particles as long as they are small enough to volatize completely in the flame.

The differences in effectiveness seen here are not large: the difference in the slopes, corrected for the heating values, between the DMMP solution and the average of the phosphorus acid solutions is 21%. Gas-phase kinetic differences may be significant compared to the remaining discrepancy between DMMP and acid solutions, as this difference in effectiveness is similar to that found between the vapor-phase compounds shown in Fig. 7. Kinetics for the aqueous phosphorus solutions tested are largely unknown so it is not possible to separate gas-phase effects from those due to the particles. However, taking the 21% difference between DMMP and the acid solution slopes as an estimate of the magnitude of the particle effects, we conclude that the net particle effect appears to be smaller than the gas-phase chemical effect of the phosphorus. Under the conditions and assumptions reported here, the particles would account for about one-quarter of the total suppression of the solution, compared with the gas-phase chemical effect that is responsible for about 40% of the total suppression. The same wall losses were assumed for all the acid solutions, and this assumption may affect the observed magnitude of the particle effect. However, some positive particle effect on suppression can be inferred even without making this assumption. Even if zero losses are assumed for the acid solutions (giving a lower bound on their effectiveness), the acid solutions are still all more effective than the DMMP solution.

Some information on differences in the gas-phase chemical effect was gained from extinction strain rate calculations. The normalized global extinction strain rate obtained from these calculations are given in Table 4. The effect of the H_2O is decoupled from that of the PCC. As seen, the calculated reduction in extinction strain rate is significantly less than that observed experimentally: the PCC alone (no H_2O included) reduces the extinction strain rate from its undoped value by only about: 1.5% for DMMP; 2.3% for phosphorous acid; and 3% for OPA. The trend in effectiveness

is similar to that seen experimentally; that is, OPA is the most effective and DMMP is the least effective PCC. However, the effectiveness is about one-fifth that seen experimentally for neat DMMP. Thus, calculations using the current chemical kinetic mechanism can be used to gain only qualitative insight into the gas-phase effect. Newer kinetic mechanisms (e.g., [27,28]) may yield better agreement, and should be investigated.

4. Summary

An investigation of the flame suppression for water, vapor-phase phosphorus-containing compounds, and residual particles derived from aqueous solutions of PCCs was performed. To do so, a technique to introduce an additive as a fine mist of droplets into an opposed-jet nonpremixed burner was developed and validated. A high-efficiency nebulizer was used to produce the droplets, and droplet size measurements using a phase-Doppler particle anemometer established that the size distribution of the droplets is independent of the compound and liquid flow rate used. This allows wide application of the HEN for studying different potential additives. Key features of the system are small droplet size, large residence time of the reactant stream under temperature-controlled conditions, and the availability of an accurate procedure for measuring losses to surfaces within the feed system. These features lead to complete evaporation of volatile constituents of the droplets, a well-characterized state of the reactant mixture at the exit of the burner tube, and well-defined gas-phase loading of added agent at the flame. A comparison of the flame suppression effectiveness of PCCs introduced into the burner system in the liquid phase is made. This experimental approach does not permit a study of the effect of droplets on the flame; however, it does allow investigation of the physical effect of residual particles formed from the evaporation of droplets.

Experimental results indicate a significant reduction in global extinction strain rate with the addition of pure water vapor (10% reduction at 1.5% molar loading), in good agreement with numerical results. With the addition of a small amount (1.6% molar) of PCC in water solution, this reduction doubles. These results support the use of water as a means of delivering a chemically active, condensed phase agent to an actual fire. They also show that the effectiveness of a PCC/water solution can be determined by a linear addition of the effectiveness of the components, over the range of concentrations and loadings reported here. Comparisons of experimental flame suppression effectiveness are made for several volatile and non-

Table 4
Summary of calculated extinction strain rates, normalized by the undoped value (a_q/a_{q0})

Dopant	Normalized extinction strain rate
DMMP	0.99
OPA	0.97
P(OH)$_3$	0.98
H$_2$O	0.88
DMMP + H$_2$O	0.87
OPA + H$_2$O	0.86
P(OH)$_3$ + H$_2$O	0.87

Note. The effect of PCCs was found using Glaude's PCC mechanism (see text for details). Quantities of dopants are: 250 ppm of PCC and/or 1.54% H_2O (molar).

volatile PCCs. Volatile PCCs all showed comparable values of effectiveness, all observably lower than those of the nonvolatile PCCs. Thus it appears that the chemical structure of the parent compound has relatively little impact on flame suppression effectiveness, while the residual particles enhance it. Despite the effect of residual particles, participation of phosphorus in the gas-phase chemistry is the primary suppression mechanism.

References

[1] C.C. Grant, NFPA J. 88 (1994) 41–54.

[2] R.E. Tapscott, T.A. Moore, J.A. Kaizerman, C.J. Kibert, R.A. Tetla, Advanced agent halon substitutes, in: Proceedings of the 1995 International CFC and Halon Alternatives Conference, Washington, DC, 1995, pp. 644–649.

[3] D. Trees, K. Seshadri, A. Hamins, in: A.W. Miziolek, W. Tsang (Eds.), Halon Replacements: Technology and Science, American Chemical Society, Washington, DC, 1995, pp. 190–203.

[4] P. Papas, J.W. Fleming, R.S. Sheinson, Proc. Combust. Inst. 26 (1997) 1405–1412.

[5] T. Mitani, Combust. Flame 44 (1982) 247–260.

[6] M. Rumminger, G. Linteris, Combust. Flame 123 (2000) 82–94.

[7] Y. Ju, C.K. Law, Proc. Combust. Inst. 28 (2000) 2913–2920.

[8] A.M. Lentati, H.K. Chelliah, Combust. Flame 115 (1998) 158–179.

[9] D. Trees, K. Seshadri, Combust. Sci. Technol. 122 (1997) 215–230.

[10] R.A. Dodding, R.F. Simmons, A. Stephens, Combust. Flame 15 (1970) 313–315.

[11] T. Mitani, Combust. Flame 50 (1983) 177–188.

[12] A. Hamins, Proc. Combust. Inst. 27 (1998) 2857–2864.

[13] T.A. Milne, C.L. Green, D.K. Benson, Combust. Flame 15 (1970) 255–264.

[14] A. Jones, P.F. Nolan, J. Loss Prevent. Proc. 8 (1995) 17–22.

[15] C.C. Ndubizu, R. Ananth, P.A. Tatem, V. Motevalli, Fire Saf. J. 31 (1998) 253–276.

[16] K. Prasad, C. Li, K. Kailasanath, C. Ndubizu, R. Ananth, P.A. Tatem, Combust. Sci. Technol. 132 (1998) 325–364.

[17] E.J.P. Zegers, B.A. Williams, R.S. Sheinson, J.W. Fleming, Proc. Combust. Inst. 28 (2000) 2931–2938.

[18] J.C. Yang, M.K. Donnelly, N.C. Prive, W.L. Grosshandler, Fire Saf. J. 36 (2001) 55–72.

[19] R. Zheng, K.N.C. Bray, B. Rogg, Combust. Sci. Technol. 126 (1997) 389–401.

[20] B. Mesli, I. Gokalp, Combust. Sci. Technol. 153 (2000) 193–211.

[21] A.K. Lazzarini, R.H. Krauss, H.K. Chelliah, G.T. Linteris, Proc. Combust. Inst. 28 (2000) 2939–2945.

[22] M.A. MacDonald, T.M. Jayaweera, E.M. Fisher, F.C. Gouldin, Combust. Flame 116 (1997) 166–176.

[23] R.T. Wainner, K.L. McNesby, R.G. Daniel, A.W. Miziolek, V.I. Babushok, Experimental and mechanistic investigation of opposed-flow propane/air flames by phosphorus-containing compounds, in: Proceedings of the 10th Halon Options Technical Working Conference, Albuquerque, NM, 2000, pp. 141–150.

[24] R.R. Skaggs, R.G. Daniel, A.W. Miziolek, K.L. McNesby, Spectroscopic studies of inhibited opposed flow propane/air flames, in: Proceedings of the First Joint Meeting of the U.S. Sections of the Combustion Institute, Washington, DC, 1999, pp. 575–579.

[25] J.W. Hastie, D.W. Bonnell, Molecular Chemistry of Inhibited Combustion Systems, National Bureau of Standards, 1980.

[26] T.M. Jayaweera, C.F. Melius, W.J. Pitz, C.K. Westbrook, O.P. Korobeinichev, V.M. Shvartsberg, A.G. Shmakov, I.V. Rybitskaya, H.J. Curran, Combust. Flame 140 (2005) 103–115.

[27] A.G. Shmakov, O.P. Korobeinichev, V.M. Shvartsberg, D.A. Knyazkov, T.A. Bolshova, I.V. Rybitskaya, Proc. Combust. Inst. 30 (2004) 2345–2352.

[28] O.P. Korobeinichev, V.M. Shvartsberg, A.G. Shmakov, T.A. Bolshova, T.M. Jayaweera, C.F. Melius, W.J. Pitz, C.K. Westbrook, H. Curran, Proc. Combust. Inst. 30 (2004) 2350–2357.

[29] A. Twarowski, Combust. Flame 94 (1993) 91–107.

[30] M.A. MacDonald, F.C. Gouldin, E.M. Fisher, Combust. Flame 124 (2001) 668–683.

[31] T.M. Jayaweera, PhD dissertation, Cornell University (2002).

[32] K. Seshadri, N. Ilincic, Combust. Flame 101 (1995) 271–294.

[33] A.R. Masri, Combust. Sci. Technol. 96 (1994) 189–212.

[34] Y. Otsuka, T. Niioka, Combust. Flame 21 (1973) 163–176.

[35] H.K. Chelliah, C.K. Law, T. Ueda, M.D. Smooke, F.A. Williams, Proc. Combust. Inst. 23 (1990) 503–511.

[36] G.F. Carrier, F.E. Fendell, F.E. Marble, SIAM J. Appl. Math. 28 (1975) 463–500.

[37] A. Linan, Acta Astronaut. 1 (1974) 1007–1039.

[38] A.E. Lutz, R.J. Kee, J.F. Grcar, F.M. Rupley, OPPDIF: A Fortran Program for Computing Opposed-Flow Diffusion Flames, Sandia National Laboratories, SAND96-8243, 1996.

[39] R.J. Kee, F.M. Rupley, J.A. Miller, Chemkin-II: A Fortran Chemical Kinetics Package for the Analysis of Gas-Phase Chemical Kinetics, Sandia National Laboratories, SAND89-8009, 1989.

[40] D.C. Rapp, M.F.M. Nogueira, E.M. Fisher, F.C. Gouldin, Environ. Eng. Sci. 14 (1997) 133–140.

[41] K. Seshadri, F. Williams, Int. J. Heat Mass Transfer 21 (1978) 251–253.

[42] I.K. Puri, K. Seshadri, Combust. Flame 65 (1986) 137–150.

[43] S. Turns, An Introduction to Combustion: Concepts and Applications, first ed., McGraw–Hill, New York, 1996.

[44] K.H. Leong, J. Aerosol Sci. 12 (1981) 417–435.

[45] S.C. Li, P.A. Libby, F.A. Williams, Combust. Flame 94 (1993) 161–177.

[46] D.E. Rosner, Y.F. Khalil, J. Aerosol Sci. 31 (2000) 273–293.

[47] P.A. Glaude, H.J. Curran, W.J. Pitz, C.K. Westbrook, Proc. Combust. Inst. 28 (2000) 1749–1756.

[48] G.P. Smith, D.M. Golden, M. Frenklach, N.W. Moriarty, B. Eiteneer, M. Goldenberg, C.T. Bowman, R.K. Hanson, S. Song, C. William, J. Gardiner, V.V. Lissianski, Z. Qin, available at: http://www.me.berkeley.edu/gri_mech/.

[49] W.M. Pitts, J.C. Yang, M.L. Huber, L.G. Blevins, Characterization and Identification of Super-Effective Thermal Fire Extinguishing Agents—First Annual Report, NISTIR 6414, 1999.

[50] M.A. MacDonald, T.M. Jayaweera, E.M. Fisher, F.C. Gouldin, Proc. Combust. Inst. 27 (1998) 2749–2756.

[51] T. Niioka, T. Mitani, M. Takahashi, Combust. Flame 50 (1983) 89–97.

[52] P.R. Bevington, Data Reduction and Error Analysis for the Physical Sciences, McGraw–Hill, New York, 1969.

[53] Z. Liu, A.K. Kim, J. Fire Protection Eng. 10 (2000) 32–50.

[54] Y. Saso, Y. Ogawa, N. Saito, H. Wang, Combust. Flame 118 (1999) 489–499.

[55] E.M. Fisher, Equilibrium composition calculations for combustion of organophosphorus compounds, in: Proceedings of the 1995 Fall Technical Meeting of the Eastern States Section of the Combustion Institute, Worcester, MA, 1995, pp. 179–182.